A Novel Multilevel Coded Modulation Scheme for Fiber Optical Channel with Nonlinear Phase Noise

Lotfollah Beygi*, Erik Agrell*, Pontus Johannisson† and Magnus Karlsson†
* Department of Signals and Systems, Chalmers University of Technology, SE-412 96 Gothenborg, Sweden
† Department of Microtechnology and Nanoscience, Chalmers University of Technology, SE-412 96 Gothenborg, Sweden

***Abstract*—A multilevel coded modulation (MLCM) system in the presence of nonlinear phase noise for fiber optical communication is introduced. The proposed scheme exploits a 16-point ring constellation with nonlinear post compensation of the self phase modulation produced via the Kerr effect. A new set partitioning based on the Ungerboeck approach is introduced to maintain unequal error protection in amplitude and phase direction. The rate allocation for the MLCM component codes for different fiber lengths and transmit powers are done numerically. Simulation results show that the proposed MLCM system provides up to 2 dB gain over a forward error correcting scheme for a block error rates around 10^{-9}, with the same overhead (7%) and complexity.**

I. Introduction

In the past few years, significant attention has been devoted to increasing the spectral efficiency of optical fiber links. Since exploiting a high order constellation is inevitable to achieve high spectral efficiency, intense efforts have been carried out to find an optimum signal constellation for data transmission in the fiber optical channels [1], [2]. Previously known signal constellations and channel coding techniques for the AWGN channel should be tailored to the impairments introduced in these links in order to achieve the high spectral efficiencies promised by the Shannon theory [3], [4].

Among the fiber-induced impairments, nonlinear phase noise (NLPN) shows a major effect particularly in long-haul transmission [5], [6]. NLPN is caused by the interaction between the signal and amplified spontaneous noise (ASE) via the fiber Kerr nonlinearity [7]. Different approaches has been investigated for combating the effect of NLPN, e.g., by optical hardware methods [8]–[10] or by electronic compensation with pre-distortion [11], [12] or post compensation [13], [14].

Lau and Kahn [14] derived a closed form expression for the decision boundaries of a PSK constellation in the presence of NLPN. Based on this analytical result, they proposed a Maximum Likelihood (ML) detector for phase modulated signals and a suboptimal detector for 16-QAM constellation.

Although this method performs close to optimal ML decoding, the NLPN in long-haul dispersion-managed fiber links seriously degrades the received signal in such a way that reliable data transmission would be impossible for very long fiber lengths. This means that the system has not only poor performance at low SNR (linear regime) but also at the nonlinear high SNR regime. This issue motivates us to study coded modulation techniques for this non-AWGN channel.

Research supported by the Swedish Research Council under grant 2007-6223.

Considering the high data rates in optical communication systems, the computational complexity plays a main role in the design of coded modulation schemes for these systems. Multilevel coded modulation (MLCM) [15] due to exploiting multistage decoding (MSD) with hard and soft decision decoding provides suitable trade-off between the complexity and performance.

In this paper, we consider the nonlinear post compensator proposed in [14] to compensate the degradation caused by NLPN for a fiber link with distributed amplifiers. Since the Euclidean distance is not a valid criterion in the design of channel coding for non-Gaussian channel, we introduce a new set partitioning algorithm for 16-point ring constellations based on the Ungerboeck approach. In this method, we accomplish the set partitioning in two steps; first in radius and then in phase direction. Numerical optimization technique is used to find the optimum rate allocation for different layers, in terms of minimizing the total block error rate (BLER).

The major difference between the proposed method and previous approaches is in the design criterion. In contrast to coded modulation schemes proposed in [16], [17], we take the non-Gaussian noise into account in the design. In comparison to the methods introduced in [18], [19] which suffer from high complexity due to exploiting iterative or soft decoding, the complexity of the proposed scheme can be lower than a system with an independent forward error correction (FEC) and modulation. We use FEC system to refer to such a system in the rest of this paper.

Moreover, the symbol error rate (SER) of the uncoded 16-point ring constellation for the suboptimal receiver of [14] in the presence of NLPN is derived analytically. In addition, it is demonstrated that the radii of the ring constellation can be chosen to achieve better performance in the highly nonlinear regime in comparison to 16-QAM, which was shown before by simulation [20].

Finally, the performance of the proposed scheme in fiber optical channels with different lengths is evaluated through simulation. The results show a significant performance gain in using an MLCM scheme over a FEC system with the same overhead. Interestingly, the MLCM scheme has a lower complexity at BLER around 10^{-9} and, at the same time, it shows 2 dB performance improvement.

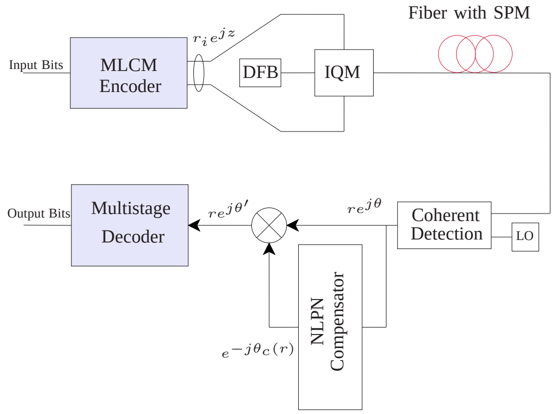

Figure 1. An MLCM scheme for a fiber link with SPM produced via the Kerr effect.

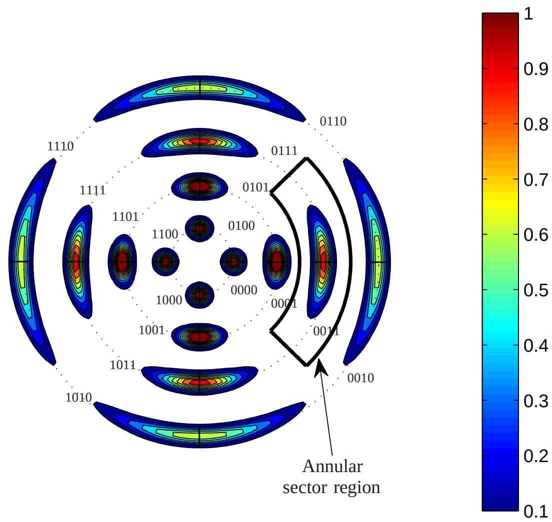

Figure 2. 16-point ring constellation with Gray labeling corrupted by NLPN for a fiber with L = 6000 km and P_t = 0 dBm (using (2), after NLPN compensator).

II. System Model

We consider a fiber optical link with SPM produced via the Kerr effect and a data transmission system exploiting a 16-point constellation with four rings as seen in Fig. 2. In the rest of paper, it is assumed that the exploited pulse shape $h(t)$ has a unit energy ($\int_{-\infty}^{\infty} h^2(t)\ \mathrm{d}t = 1$). The vector (r_1, r_2, r_3, r_4) represents the radii distribution of this constellation in such a way that $\sum_{i=1}^{4} r_i^2 = 4P_\mathrm{t}$, where P_t is the average transmitted power. According to the proposed block diagram of Fig. 1, the MLCM unit produces complex I/Q symbol $r_i e^{jz}$, where $1 \leq i \leq 4$ and $z \in \{0, \frac{\pi}{2}, \pi, \frac{3\pi}{2}\}$. The optical I/Q modulator (IQM), transforms the generated complex symbol to an I/Q modulated signal.

The optical channel considered in this model is a fiber link of total length L with distributed amplification, where the fiber loss is completely compensated for by this amplification [14]. The ASE noise generated by inline amplifiers is modeled as complex zero-mean circularly symmetric Gaussian random variables with variance

$$\sigma^2 = 2n_{sp}h\nu\Delta\nu\alpha L, \tag{1}$$

in two polarizations, where $\Delta\nu = 42.7$ GHz is the bandwidth of the optical filter at the receiver, $n_{sp} = 1.41$ [14] is the spontaneous emission factor, $h\nu$ is the photon energy, which at wavelength of 1550 nm is $1.28 \times 10^{-19}[J]$ and $\alpha = 0.25$ dB/km is the attenuation coefficient. In this paper, we consider only the noise within a receiver matched filter, i.e., ignoring Kerr effect induced nonlinearity from out of band signals and noises similar to [13] and [14].

The pulse shape is nonreturn-to-zero (NRZ) with an MLCM scheme of 42.7 Gsymbol/s to support an information bit rate of 160 Gb/s with 7% added redundancy of the coded modulation scheme. Moreover, due to the lack of an analytical expression for the joint probability density function of the amplitude and the phase of the received signal for a fiber channel with chromatic dispersion and nonlinearity and besides for the simplicity of the analysis, we neglect the effect of chromatic dispersion.

We define the received amplitude r as the amplitude of the received electric field at the output of the coherent receiver, divided by σ. The amplitude-dependent phase rotation $\theta_c(r)$ (caused by SPM) of the received signal is removed by the nonlinear maximum likelihood NLPN compensator of [14], as shown in Fig. 1. Finally the compensated received signal is used by an MLCM multistage decoder to extract the transmitted information bits. Here, using the results of [14], the joint probability density function (pdf) of the signal's normalized amplitude (r) and compensated phase (θ') for a transmitted symbol from an M-PSK constellation with initial phase θ_0 and radius $\sqrt{\xi}$, is obtained by

$$f_{R,\Theta'}(r,\theta') = \frac{f_R(r,\xi)}{2\pi} + \frac{1}{\pi}\sum_{m=1}^{\infty} |C_m(r)| \cos\left[m\left(\theta' - \theta_0\right)\right], \tag{2}$$

where

$$f_R(r,\xi) = 2r\exp\left[-\left(r^2 + \rho_s\right)\right] I_0\left(2r\sqrt{\rho_s}\right), \tag{3}$$

is the Ricean pdf of the received amplitude and $\rho_s = \xi/\sigma^2$ is the signal-to-noise ratio (SNR). The Fourier coefficient $C_m(r)$ is [14]

$$C_m(r) = \frac{r\sec(\sqrt{jmx})}{s_m} e^{\rho_s\sqrt{jmx}\tan\sqrt{jmx}} e^{-\frac{r^2+\alpha_m^2}{2s_m}} I_m\left(\frac{\alpha_m r}{s_m}\right),$$

where

$$x = \frac{\gamma\xi L}{\rho_s + 1/2}, \quad \alpha_m = \sqrt{\rho_s}\sec\sqrt{jmx}, \quad s_m = \frac{\tan\sqrt{jmx}}{2\sqrt{jmx}},$$

$I_m(\cdot)$ denotes the m^{th}-order modified Bessel function of the first kind, and $\gamma = 1.2\ \mathrm{W}^{-1}\mathrm{km}^{-1}$ is the nonlinear coefficient of the fiber.

III. SER of a Uncoded 16-point Ring Constellation

Considering the NLPN impairment of the fiber optical channel, the noise in the phase and radial direction will be different. In this section, we analyze the SER of a 16-point ring constellation exploiting the suboptimal decoder proposed in [14]. In this detection method, the annular sector (a sector in the area between the two concentric circles or a flat ring-shaped area, see Fig. 2) is used instead of the exact Voronoi region as the decision region in the detector. Since the distribution of noise in the radial direction is Ricean, the ML decision boundaries between rings are obtained by intersecting the two Ricean pdf's

$$f_R(\mu_i, r_i^2) = f_R(\mu_i, r_{i+1}^2),$$

where μ_i is the radius of circle which is the ML decision boundary between rings i and $i+1$, normalized by σ. By using $I_0(x) \approx \exp(x)/\sqrt{2\pi x}$ for high SNR ($|x| \gg 1$), we obtain

$$\mu_i = \frac{r_i + r_{i+1}}{2\sigma} + \frac{1}{2}\frac{\ln r_i - \ln r_{i+1}}{r_i - r_{i+1}}\sigma; \quad i = 1, \dots, 3$$

where $\ln$ is the natural logarithm. Here, we compute the probability of correct detection of a transmitted symbol $s = r_i e^{j0}$ selected from ring i and initial phase $\theta_0 = 0$ by

$$P_{c_i} = \Pr\left\{R \in [\mu_{i-1}\ \mu_i) \wedge \Theta' \in [-\frac{\pi}{4}\ \frac{\pi}{4})\right\},$$

where $i = 1, \dots, 4$, $\mu_0 = 0$ and $\mu_4 = \infty$. This probability can be computed by taking the integral of (2) over the annular sector of the symbols in different rings i. Therefore, using the symmetry of the ring constellation, it is readily seen that the total SER of the 16-point ring constellation is

$$\text{SER} = 1 - \frac{1}{4}\sum_{i=1}^{4} P_{c_i}.$$

Eventually we obtain

$$\text{SER} = 1 - \frac{1}{4}\sum_{i=1}^{4}\left(\frac{P_{r_i}}{4} + \sum_{m=1}^{\infty}\frac{2\eta_{m,i}}{m\pi}\sin\left(\frac{m\pi}{4}\right)\right), \tag{4}$$

where

$$P_{r_i} = Q\left(\sqrt{2}\frac{r_i}{\sigma}, \sqrt{2}\mu_{i-1}\right) - Q\left(\sqrt{2}\frac{r_i}{\sigma}, \sqrt{2}\mu_i\right), \tag{5}$$

$$\eta_{m,i} = \int_{\mu_{i-1}}^{\mu_i} |C_m(r)| \mathrm{d}r,$$

and $Q(x,y)$ is the Marcum Q function in (5), which is defined by

$$Q(x,y) = \int_{y}^{\infty} t \exp\left(-\frac{t^2 + x^2}{2}\right) I_0(xt) \mathrm{d}t.$$

IV. Optimized MLCM scheme for NLPN

We assume that the MLCM component codes are selected from t_i-error correcting Reed–Solomon (RS) codes [21, Ch. 7] over the Galois field $GF(2^8)$ with 2^8 elements and length $n = 8 \times (2^8 - 1)$ bits. As shown in Fig. 3, a block of information bits $\underline{u}$ is demultiplexed into four blocks $\underline{u}_1, \dots, \underline{u}_4$ in such a way that the length of $\underline{u}_i$ is nR_i ($1 \le i \le 4$) where R_i is the code rate of component code i. The component codes RS-Enc1, …, RS-Enc4 encode the information bit blocks to code vectors $\underline{v}_1, \dots, \underline{v}_4$ with identical length n.

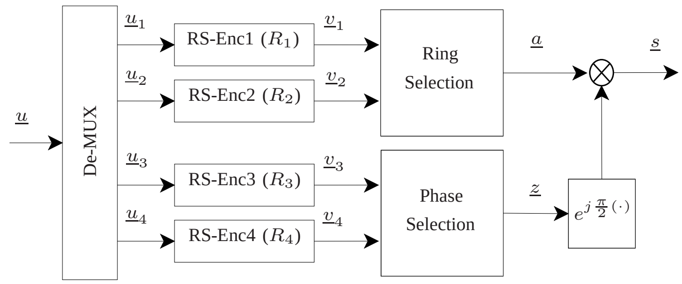

Figure 3. The MLCM Encoder with four RS component codes with rates $R_1, \dots, R_4$.

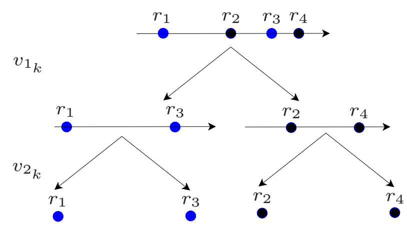

Figure 4. Radius set partitioning of the ring constellation.

The labeling in Fig. 2 lets us map four bits to a symbol from the 16-point ring constellation in two steps. For each bit instance k, we have four bits $v_{1_k} v_{2_k} v_{3_k} v_{4_k}$ to be mapped to a symbol s_k. The mapping is done by selecting $s_k = a_k e^{jz_k}$, where $a_k \in \{r_1, \dots, r_4\}$ is determined by $v_{1_k} v_{2_k}$ and $z_k \in \{0, \frac{\pi}{2}, \pi, \frac{3\pi}{2}\}$ is determined by $v_{3_k} v_{4_k}$.

We proceed with the design of the MLCM scheme to protect different layers unequally, i.e., the higher probability of error, the higher error protection should be assigned. We need to compute the average bit error probability of each layer to clarify the amount of protection, based on the vulnerability of each layer against error. The final step of the mapping operation is to define the ring and phase selection units (as shown in Fig. 3). This mapping is accomplished by the set partitioning of the ring constellation in two steps.

A. Set partitioning in radial direction

The set partitioning in the radial direction is defined in Fig. 4. The Ungerboeck set partitioning [22] approach is used to choose one ring corresponding to the bits $v_{1_k} v_{2_k}$. In layer 1, corresponding to value of v_1, 0 or 1, one of the subsets $A_1 = \{r_1, r_3\}$ or $A_2 = \{r_2, r_4\}$ is selected. Therefore the average uncoded bit error probability of layer 1 is

$$P_1 = \frac{1}{2}\left(\Pr\{\hat{a}_k \in A_2 \mid a_k \in A_1\} + \Pr\{\hat{a}_k \in A_1 \mid a_k \in A_2\}\right),$$

where $\hat{a}_k$ is the detected ring using a hard decision detector for the transmitted symbol from ring a_k, and

$$\Pr\{\hat{a}_k \in A_2 \mid a_k \in A_1\} = \frac{1}{2}\Pr\{\hat{a}_k \in A_2 \mid a_k = r_1\} + \frac{1}{2}\Pr\{\hat{a}_k \in A_2 \mid a_k \in r_3\}. \quad (6)$$

The two terms in the right hand side of (6) can be easily computed considering the Ricean distribution of the received amplitude r given in (3) and eventually we obtain

$$\Pr\{\hat{a}_k \in A_2 \mid a_k \in A_1\} = \frac{1}{2}\sum_{i=0}^{1}\big[Q(\sqrt{2}\frac{r_{2i+1}}{\sigma}, \sqrt{2}\mu_1) - Q(\sqrt{2}\frac{r_{2i+1}}{\sigma}, \sqrt{2}\mu_2) + Q(\sqrt{2}\frac{r_{2i+1}}{\sigma}, \sqrt{2}\mu_3)\big], \quad (7)$$

and

$$\Pr\{\hat{a}_k \in A_1 \mid a_k \in A_2\} = \frac{1}{2}\sum_{i=1}^{2}\big[1 - Q(\sqrt{2}\frac{r_{2i}}{\sigma}, \sqrt{2}\mu_1) + Q(\sqrt{2}\frac{r_{2i}}{\sigma}, \sqrt{2}\mu_2) - Q(\sqrt{2}\frac{r_{2i}}{\sigma}, \sqrt{2}\mu_3)\big]. \quad (8)$$

An analogous analysis can be applied to compute the average uncoded bit error probability of layer 2

$$P_2 = \frac{1}{2}\Pr\{\hat{a}_k \neq a_k | a_k \in A_1\} + \frac{1}{2}\Pr\{\hat{a}_k \neq a_k | a_k \in A_2\},$$

where

$$\Pr\{\hat{a}_k \neq a_k \mid a_k \in A_1\} = \frac{1}{2}\big[Q(\sqrt{2}\frac{r_1}{\sigma}, \sqrt{2}\mu_1') + 1 - Q(\sqrt{2}\frac{r_3}{\sigma}, \sqrt{2}\mu_1')\big], \quad (9)$$

and

$$\Pr\{\hat{a}_k \neq a_k \mid a_k \in A_2\} = \frac{1}{2}\big[Q(\sqrt{2}\frac{r_2}{\sigma}, \sqrt{2}\mu_2') + 1 - Q(\sqrt{2}\frac{r_4}{\sigma}, \sqrt{2}\mu_2')\big]. \quad (10)$$

In (9) and (10), μ_1' and μ_2' are the radii of the circles which are the ML decision boundaries between rings (1,3) and (2,4), respectively.

B. Set partitioning in phase direction

The phase selection unit rotates the selected point from each ring corresponding to the two bits $v_{3_k}v_{4_k}$, using the Ungerboeck set partitioning shown in Fig. 5. In the error probability of layer 1 and 2 in the radial direction, the nonlinearity does not have any significant contribution while the dominant effect (especially at high SNR) in layer 3 and 4 is due to NLPN. Following the same approach as in the previous layers and using the symmetry of the ring constellation in the phase direction, one may define two subsets $B_1 = \{0, \pi\}$ and $B_2 = \{\frac{\pi}{2}, \frac{3\pi}{2}\}$ and hence

$$P_3 = \frac{1}{4}\sum_{i=1}^{4}\Pr\{\hat{z}_k \in B_2 \mid z_k \in B_1 \wedge a_k = r_i\}, \quad (11)$$

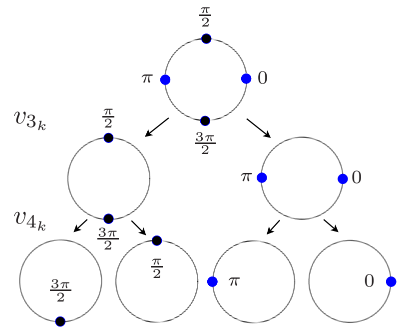

Figure 5. Phase set partitioning of the ring constellation.

where $\hat{z}_k$ is the detected phase using a hard decision detector for the transmitted symbol with phase z_k. The conditional pdf $f_{\Theta'|R}(\theta' \mid r)$ can easily be computed by exploiting (2), (3) and the Bayes' rule, and then following an analogous approach as in (6), (7) and (8), we obtain

$$\Pr\{\hat{z}_k \in B_2 \mid z_k \in B_1 \wedge a_k = r_i\} = \frac{1}{2} + \frac{1}{P_{r_i}}\sum_{m=1}^{\infty}\frac{2\eta_{m,i}}{m\pi}\left(\sin\left(\frac{3m\pi}{4}\right) - \sin\left(\frac{m\pi}{4}\right)\right). \quad (12)$$

Finally, considering the symmetry of the constellation for symbols inside each ring, the average bit error probability of layer 4 is obtained by

$$P_4 = \frac{1}{4}\sum_{i=1}^{4}\Pr\{\hat{z}_k \neq 0 \mid z_k = 0 \wedge a_k = r_i\}, \quad (13)$$

where

$$\Pr\{\hat{z}_k \neq 0 | z_k = 0, a_k = r_i\} = \frac{1}{2} - \frac{1}{P_{r_i}}\sum_{m=1}^{\infty}\frac{2\eta_{m,i}}{m\pi}\sin\left(\frac{m\pi}{2}\right).$$

V. Rate Allocation of the MLCM Scheme

Increasing the minimum Euclidean distance between different generated blocks of symbols $\underline{s}$ at the modulator output (see Fig. 1) is the design rule of the MLCM approach [15] for AWGN channels, while this criterion is not valid anymore to reach the best performance in the channels with non-Gaussian noise. Therefore, we proceed with the design of the MLCM scheme by minimizing the total BLER of the system subject to a given total rate $R = 0.9294$ (about 7% overhead). In other words, one should find code rates R_i, $i = 1, \ldots, 4$ that minimize the total BLER of the MLCM system. After derivation of the uncoded bit error probability of the layers $P_1, ..., P_4$, the BLER (a block contains $k = 4nR$ information bits) of the system can be computed by

$$P_\mathrm{e} = 1 - \prod_{l=1}^{4}(1 - P_{Bl}), \quad (14)$$

where P_{Bl} is the block error probability of layer l, which contains $k_l = nR_l$ information bits, conditioned on the fact that there is no error in layers $1, \ldots, l-1$ and $\sum_{l=1}^{4} k_l =$

k; $R = \frac{k}{4n}$. By some algebraic manipulations, we obtain

$$P_{\text{e}} = \sum_{l=1}^{4} P_{Bl} - \sum_{i=1}^{4} \sum_{\substack{j=1 \\ j \neq i}}^{4} P_{Bi} P_{Bj} + \ldots \tag{15}$$

For moderate SNR (SER $< 10^{-2}$), P_e can be approximated very well by using only the first term of (15). Thus the problem is reduced to minimizing

$$P_{\text{e}} \approx \sum_{l=1}^{4} P_{Bl}, \tag{16}$$

subject to the constraint $\frac{1}{4}\sum_{l=1}^{4} R_l = R$. We change the code rate constraint to the correcting capability constraint, to express P_{Bl} as a function of the the correcting capability t_l of the component code l by the union bound. The BLER for layer $l = 1, \ldots, 4$ of an MLCM system with hard decision MSD can be approximated based on the union bound

$$P_{Bl} \leq \sum_{i=t_l+1}^{n} \binom{n}{i} P_l^i (1 - P_l)^{n-i}. \tag{17}$$

By substituting (17) into (16), eventually we obtain the total BLER of the MLCM scheme

$$P_{\text{e}} = \sum_{l=1}^{4} \sum_{i=t_l+1}^{n} \binom{n}{i} P_l^i (1 - P_l)^{n-i}. \tag{18}$$

The minimization of (18) can be accomplished numerically subject to

$$\frac{1}{4} \sum_{l=1}^{4} t_l = T, \tag{19}$$

where $T = n(1 - R)/4$. Table I shows the result of the rate allocation for the MLCM layers based on minimizing the total BLER for hard decision MSD, by numerical optimization for a fiber length of 6000 km.

VI. Simulation Results

In this section, we evaluate the performance of the proposed MLCM scheme for the fiber optical channel with specification given in section II. For this purpose, we compare the BLER performances of the MLCM scheme with a FEC system considering the same total rate $R = 0.929$ and a 16-point ring constellation. For a fair comparison, the component codes are chosen from the RS codes over GF(2^8) with the same length $n = 2040$ bits.

The Gray mapping in Fig. 2 for mapping four bits to a constellation point is used for the FEC system. The radii of the ring constellation are selected by a numerical search method as $(0.28, 0.66, 1.06, 1.53)\sqrt{P_t}$ to reach the minimum SER for uncoded data transmission in the nonlinear regime (high transmit power). Since this MLCM scheme can be applied to arbitrary radii distributions, we leave this radii optimization problem for future study.

The optimum rate allocation of the MLCM layers using [23] is shown in Fig. 6 for distance $L = 5000$ km. This simulation

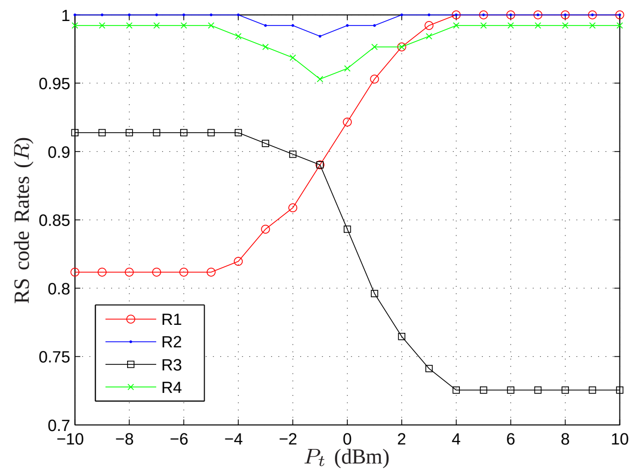

Figure 6. Optimum rate allocation of MLCM RS component codes for $L = 5000$ km .

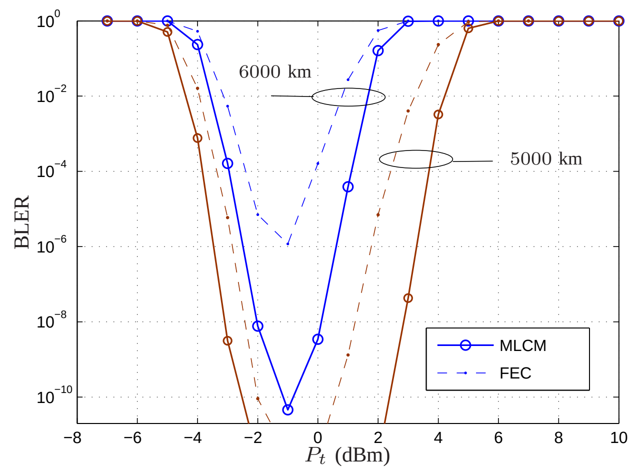

Figure 7. BLER of a system with a 16-point ring constellation and RS component codes for $L = 5000$ km and 6000 km fiber links with NLPN.

confirms that layer 1 is more vulnerable to errors at low SNR while layer 3 needs more protection at high SNR. As seen in Fig. 7, the MLCM scheme improves the performance of the system in both the linear and non-linear regime. Surprisingly, as seen in Figs. 6 and 7, MLCM outperforms not only in coding gain but also in decreasing the complexity of system in the nonlinear regime. For example at a transmit power of 2 dBm, R_2 =1 and hence, MLCM solely needs three RS component codes, while the FEC system requires to run one RS component code four times for the same block length of data ($k = 4 \times 1895$ bits), moreover 2 dB coding gain can be achieved by using the MLCM approach at this transmit power. In the linear regime, e.g., at a transmit power of -1.5 dBm, the MLCM system is superior to the FEC scheme by 2 dB with almost the same complexity.

The performance comparison between a 16-QAM constellation with equally spaced phase (changing the phase of the symbols in the middle ring to be equally spaced on $[0\ 2\pi)$)

Table I
RS CODE CORRECTING CAPABILITIES AND CODE RATES OF AN MLCM SYSTEM WITH HARD DECISION MSD, TOTAL CODE RATE $R = 0.929$, AND 16-POINT RING CONSTELLATION IN A FIBER LINK WITH $L = 6000$ KM.

P_t (dBm)	–5	–2	2	4
$\{t_1, \ldots, t_4\}$	$\{24, 0, 11, 1\}$	$\{12, 1, 21, 2\}$	$\{2, 0, 32, 2\}$	$\{2, 0, 32, 2\}$
$\{R_1, \ldots, R_4\}$	$\{0.81, 1, 0.91, 0.99\}$	$\{0.91, 0.99, 0.84, 0.98\}$	$\{0.98, 1, 0.77, 0.98\}$	$\{0.98, 1, 0.75, 0.98\}$

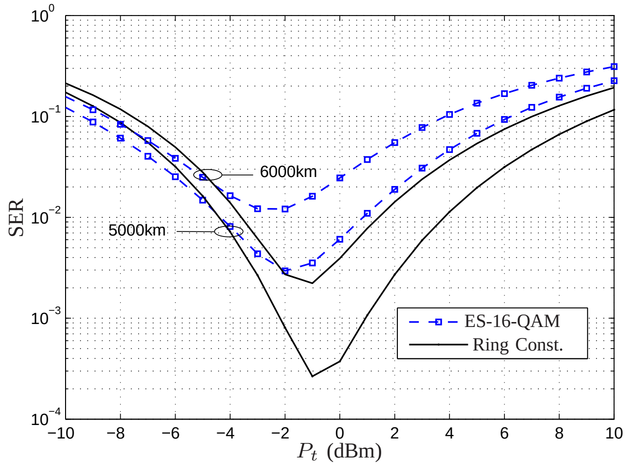

Figure 8. SER comparison of equally spaced 16-QAM (ES-16-QAM) and ring constellation for fiber lengths of 5000 and 6000 km.

[13] and the 16-point ring constellation is shown in Fig. 8. As expected, 16-QAM outperforms the ring constellation at low SNRs, while the ring constellation shows a significant performance improvement in the nonlinear regime. The radii distribution of the ring constellation is assumed fixed for all the comparisons.

VII. CONCLUSION

We designed a tailored MLCM system to a non-Gaussian fiber optical channel with nonlinear phase noise. Unequal error protection in the phase and radial direction is exploited to optimize the performance (BLER) of the system. It is shown that the MLCM system can give better performance with lower complexity. Therefore the MLCM scheme provides the possibility of reliable data transmission in a longer fiber or at a higher spectral efficiency, i.e., increasing the order of the constellation above 16 points for a fixed fiber length, in comparison to a FEC system.

REFERENCES

[1] E. Agrell and M. Karlsson, "Power-efficient modulation formats in coherent transmission systems," *J. Lightw. Technol.*, vol. 27, no. 22, pp. 5115–5126, Nov. 2009.

[2] E. Ip, A. P. T. Lau, D. J. F. Barros, and J. M. Kahn, "Coherent detection in optical fiber systems," *Opt. Express*, vol. 16, no. 2, pp. 753–791, 2008.

[3] R. J. Essiambre, G. Kramer, P. J. Winzer, G. J. Foschini, and B. Goebel, "Capacity limits of optical fiber networks," *J. Lightw. Technol.*, vol. 28, no. 4, pp. 662–701, Feb. 2010.

[4] A. D. Ellis, J. Zhao, and D. Cotter, "Approaching the non-linear Shannon limit," *J. Lightw. Technol.*, vol. 28, no. 4, pp. 423–433, Feb. 2010.

[5] J. Renaudier and G. Charlet, "Coherent detection for long haul transmission systems," *IEEE Laser, Electro-Optics Society Annual Meeting*, pp. 214–215, Oct. 2007.

[6] W. T. Anderson, L. Liu, Y. Cai, A. Pilipetskii, J. X. Cai, M. Vaa, M. Nissov, and D. Kovsh, "Modeling RZ-DPSK transmission-simulations and measurements for an installed submarine system," *Optical Fiber Communication Conference, CA*, Mar. 2005, Paper OThC1.

[7] J. P. Gordon and L. F. Mollenauer, "Phase noise in photonic communications systems using linear amplifiers," *IEEE Photon. Technol. Lett.*, vol. 15, no. 23, pp. 1351–1353, 1990.

[8] A. Mecozzi, "On the optimization of the gain distribution of transmission lines with unequal amplifier spacing," *IEEE Photon. Technol. Lett.*, vol. 10, no. 7, pp. 1033–1035, July 1998.

[9] H. Wei and D. Plant, "Simultaneous nonlinearity suppression and wide-band dispersion compensation using optical phase conjugation," *Opt. Express*, vol. 12, no. 9, pp. 1938–1958, 2004.

[10] A. P. T. Lau and J. M. Kahn, "Design of inline amplifier gains and spacings to minimize the phase noise in optical transmission systems," *J. Lightw. Technol.*, vol. 24, no. 3, pp. 1334–1341, 2006.

[11] X. Liu and D. A. Fishman, "A fast and reliable algorithm for electronic pre-equalization of SPM and chromatic dispersion," *Optical Fiber Communication Conference*, 2006, Paper OThD4.

[12] R. Waegemans, S. Herbst, L. Holbein, P. Watts, P. Bayvel, C. Fürst, and R. I. Killey, "10.7 Gb/s electronic predistortion transmitter using commercial FPGAs and D/A converters implementing real-time DSP for chromatic dispersion and SPM compensation," *Opt. Express*, vol. 17, no. 10, pp. 8630–8640, 2009.

[13] K. P. Ho and J. M. Kahn, "Electronic compensation technique to mitigate nonlinear phase noise," *J. Lightw. Technol.*, vol. 22, no. 3, pp. 779–783, Mar. 2004.

[14] A. P. T. Lau and J. M. Kahn, "Signal design and detection in presence of nonlinear phase noise," *J. Lightw. Technol.*, vol. 25, no. 10, pp. 3008–3016, Oct. 2007.

[15] H. Imai and S. Hirakawa, "A new multilevel coding method using error correcting codes," *IEEE Trans. Inf. Theory*, vol. 23, pp. 371–377, May 1977.

[16] I. B. Djordjevic, M. Cvijetic, L. Xu, and T. Wang, "Using LDPC-coded modulation and coherent detection for ultra highspeed optical transmission," *J. Lightw. Technol.*, vol. 25, no. 11, pp. 3619–3625, Nov. 2007.

[17] H. Zhao, E. Agrell, and M. Karlsson, "Trellis-coded modulation in PSK and DPSK communications," *European Conference on Optical Communications*, Sept. 2006.

[18] I. B. Djordjevic, H. G. Batshon, L. Xu, , and T. Wang, "Coded polarization-multiplexed iterative polar modulation (PM-IPM) for beyond 400 Gb/s serial optical transmission," *Conference on Optical Fiber Communication*, Mar. 2010, Paper OMK2.

[19] H. G. Batshon, I. B. Djordjevic, L. L. Minkov, L. Xu, T. Wang, and M. Cvijetic, "Proposal to achieve 1 Tb/s per wavelength transmission using three-dimensional LDPC-coded modulation," *IEEE Photon. Technol. Lett.*, vol. 20, no. 9, pp. 721–723, May 2008.

[20] M. C. Niaz and L. Beygi, "Optimization of 16-QAM constellation in the presence of nonlinear phase noise," *International Conference on Frontiers of Information Technology, Pakistan*, Dec. 2009.

[21] S. Lin and D. J. Costello, Jr., *Error Control Coding*, 2nd ed. Prentice-Hall, 2004.

[22] G. Ungerboeck, "Channel coding with multilevel/phase signals," *IEEE Trans. Inf. Theory*, vol. 28, no. 1, pp. 55–67, Jan. 1982.

[23] L. Beygi, E. Agrell, M. Karlsson, and B. Makki, "A novel rate allocation method for multilevel coded modulation," *IEEE Int. Symp. on Inf. Theory*, June 2010.